# Continuous Affinity Protein Separation with Dynamic Electrochemical Membranes

**Zhiqiang Chen, Tao Chen, Xinghua Sun , Bruce. J. Hinds***

Department of Materials Science and Engineering, University of Washington, Seattle WA **NSF CBET #1460922**

## Introduction

The downstream protein separation and purification cost can be as high as 80% of the total cost of the recombinant therapeutics protein production [1]. Immobilized metal ion affinity chromatography (IMAC) for affinity protein separation is most widely used but suffers from limitations of expense, slow complex binding, purge, desorption cycles, long intra-particle diffusion time and column regeneration.[2] Affinity membrane chromatography with convection flow through the functionalized pores improve mass transport to binding site but has low binding capacity area (thin membranes) thus requiring numerous binding/purge/release cycles and suffers from indiscriminate flow induced fouling[3]. Electrophoresis through inorganic nanoporous membranes has been used for non-affinity protein separation but still suffers from poor selectivity/fouling of sized-based exclusion for proteins of the same charge. [4-5] Needed is a transformative idea in membranes that selectively bind proteins to pore entrance and pumps them through a membrane in a continuous manner.

## Objectives

1. Producing multi-electrode membranes with protein receptor chemistry at 10nm diameter pores entrance.
2. Demonstrating continuous affinity protein separation using repeated binding and release/pumping electrophoretic voltage pulses.

## AAO Membrane Electrode Pore Entrance Size Control

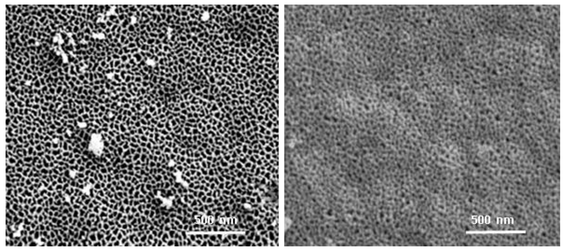


**Bare AAO membranes SEM image** **Electroless-plating AAO SEM image**

A 5 nm gold seed layer was sputtered on top of AAO membrane for subsequent gold electroless-plating [6, 7].

Oxidation reaction $C_6H_8O_6 \longrightarrow C_6H_6O_6 + 2e^- + 2H^+$

Reduction reaction $Au(S_2O_3)_2^{3-} + e^- \rightleftharpoons Au + 2S_2O_3^{2-}$

The pore diameter can be controlled by changing plating time.

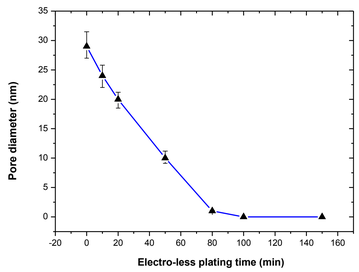


Average pore diameter of AAO membrane after different electro-less plating time

## Electrochemical Functionalization

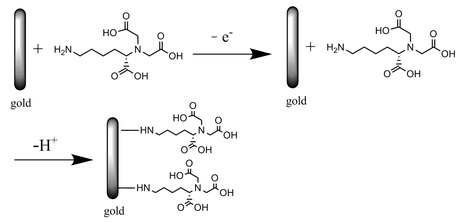


**Nα,Nα-Bis(carboxymethyl)-L-lysine (NTA) electrochemical oxidation grafting process [8].NTA binds to $Ni^{2+}$ that reversibly binds to his-tagged protein**

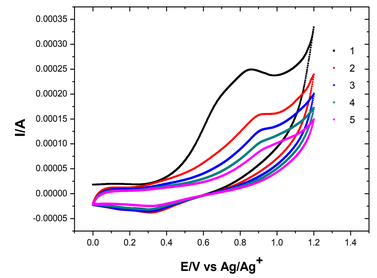


**Cyclic Voltammograms on the upper side of gold/AAO membrane in $LiClO_4$ ethanol solution with10 mM NTA for different cycles. Scan rate is 10mv/s. The oxidation potential is about 0.85V.**

## Demonstration of Membrane Functionalization

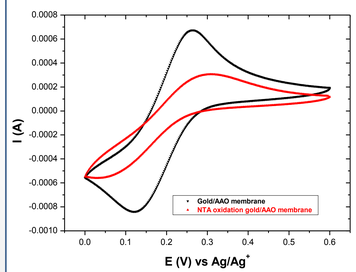


**Cyclic Voltammograms on bare and NTA oxidation AAO membrane in 0.1M $K_3Fe(CN)_6$ PBS solution. Scan rate is 100mv/s.**

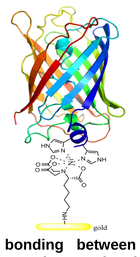


**Affinity bonding between His-tagged proteins and Ni-NTA-gold. Ni-NTA-gold was achieved by incubating the NTA-gold membrane in 0.1M $NiCl_2$ solution.**

## Gate Keeper Blocking of Functionalized Membrane

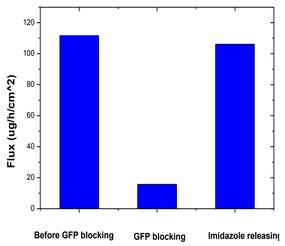


**Electrophoretic pumping flux of BSA before, after his-tagged GFP blocking the pore and after imidazole releasing the GFP. Imidazole can occupy the nickel coordination sites, displacing the his-tagged GFP [9]**

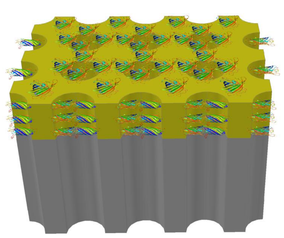

**Schematic of pore entrance blocked by His-tagged GFP in a sequential manner.**

## Direct Electrophoretic Pumping Process

**Table 1.** Electrophoretic flux and Mobility of Texas-BSA and His-tagged GFP proteins through Ni-NTA-Gold/AAO membrane at different imidazole release agent concentration

| | 10 mM imidazole | 1 mM imidazole | 0.1 mM imidazole |
|---|---|---|---|
| **BSA flux (ug $h^{-1}$ $cm^{-2}$), $f_b$** | 0.30 | 0.12 | 0.01 |
| **GFP flux (ug $h^{-1}$ $cm^{-2}$), $f_g$** | 0.28 | 0.19 | 0.082 |
| **BSA effective mobility ($10^{-6}cm^2$ $s^{-1}$ $V^{-1}$), $u_b$** | 1.97 | 0.79 | 0.07 |
| **GFP effective mobility ($10^{-6}cm^2$ $s^{-1}$ $V^{-1}$), $u_g$** | 1.88 | 1.27 | 0.54 |
| **Selectivity, S= $u_g/u_b$** | 0.95 | 1.6 | 7.7 |

(1) The pore is mostly open at high imidazole concentration, showing high flux but no selectivity since GFP is not bound to receptor.
(2) The pore is mostly blocked by His-tagged GFP at low imidazole concentration, showing good selectivity while low flux. The ideal separation factor for 1:1 ratio with a monolayer 'gate keeper' release is 1.5. Observed separation factor of 7.7 proves multiple GFPs are in the channel and some remain to block pore as GFP is released/pumped.
(3) Pulsed electrophoretic pumping with binding/pumping cycle can solve the tradeoff challenge between flux and selectivity.

## Pulse Electrophoretic Pumping Process

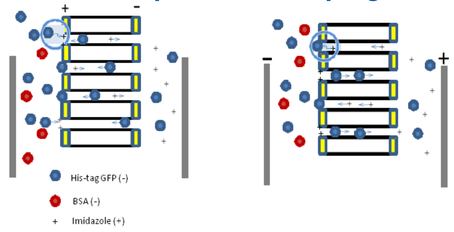


**Schematic of pulse electrophoresis process across AAO membrane**

**(1) Binding cycle:** By applying an opposite voltage across the AAO membrane, the imidazole at the feed pore is repelled and His-tagged GFP specifically bind and block the pores.

**(2) Release and pumping cycle:** Imidazole from the permeate solution is pumped to the feed solution to release the His-tagged GFP, which acts steric hindrance at the pore entrance. The released His-tagged GFP is selectively electrophoretic pumped to the permeate solution

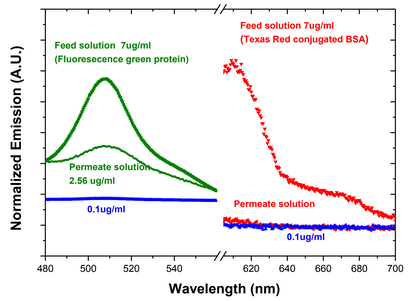


**Fluorescence spectra showing the emission intensity of the feed and permeate solutions after pulse electrophoresis. The release and pumping cycle time is 14s, the biding cycle time is 1s. The concentration of imidazole in the permeate solution is 10 mM**

**Table 2.** Electrophoretic Mobility and flux of BSA and His-tagged GFP proteins through different pumping process. The imidazole concentration in the permeate side is 10 mM

| | Gold/AAO membrane, direct pumping[a], | Ni-NTA-Gold/AAO membrane, direct pumping[a] | Ni-NTA-Gold/AAO membrane, pulse pumping (1:100)[a] | Ni-NTA-Gold/AAO membrane, pulse pumping (1:1)[b] |
|---|---|---|---|---|
| **BSA flux (ug $h^{-1}$ $cm^{-2}$), $f_b$** | 112.56 | 48.32 | 14.07 | 0.02 |
| **GFP flux (ug $h^{-1}$ $cm^{-2}$), $f_g$** | 0.7306 | 0.34 | 1.29 | 0.32 |
| **BSA effective mobility ($10^{-6}cm^2$ $s^{-1}$ $V^{-1}$), $u_b$** | 5.2 | 2.2 | 0.65 | 0.13 |
| **GFP effective mobility ($10^{-6}cm^2$ $s^{-1}$ $V^{-1}$), $u_g$** | 3.4 | 1.6 | 6.0 | 2.12 |
| **Selectivity, S= $u_g/u_b$** | 0.65 | 0.73 | 9.23 | **16** |

[a] The concentration ratio of GFP: BSA in the feed solution is 100:1. [b] The concentration ratio of GFP: BSA in the feed solution is 1:1.

(1) GFP:BSA separations as high as 16 are seen. In more realistic 1:100 feed solution, separation factor of ~9 is seen. Bound GFP generally block pores but if open, the BSA has 100 fold higher chance of entering pore.
(2) Further work to optimize blocking of non-his tagged proteins is being explored. Optimization of Binding/Release cycle may allow his-tag blocking of pore at all times.

## Conclusions

- The asymmetric nature of the commercial AAO membranes allows thin 10 nm diameter porous electrode layer to act as gate keeper while bulk 200 nm diameter channels provides high flux during the separation process.
- His-tagged proteins bound to pore entrance block other proteins in a sequential/hopping manner, allowing selective transport. Electrophoretic pumping eliminates fouling associated with pressure flow, while pores closed by gatekeeper prevents fouling by other charged proteins.
- Pulsed electrophoresis binding/release/pumping cycle allows for a continuous protein separation process. This would revolutionize protein separations where expressed proteins can be directly removed from fermentation baths with this membrane separation system.

## References

(1) Ghosh R, Cui Z.F. Protein purification by ultrafiltration with pre-treated membrane. Journal of Membrane Science. 2000, 167, 47–53.
(2) Ghosh R. Protein separation using membrane chromatography: opportunities and challenges. Journal of Chromotography A. 2002, 952, 13-17.
(3) Jain P *et al*. Protein Purification with Polymeric Affinity Membranes Containing Functionalized Poly(acid) Brushes. Biomacromolecules. 2010,11, 1019-1026.
(4) Sun X *et al.* Electrophoretic Transport of Biomolecules through Carbon Nanotube Membranes. Langmuir. 2011,27, 3150-3156.
(5) Yu S *et al.* Electrophoretic Protein Transport in Gold Nanotube Membranes. Anal. Chem. 2003, 75, 1239-1244
(6) Lam P *et al*. Electroless Gold Plating of 316 L Stainless Steel Beads. J. Electrochem. Soc.,1999,146,2517-2521
(7) Wirtz M *et al*. Template synthesized gold nanotube membranes for chemical separations and sensing. Analyst. 2002, 127,871-879.
(8) Liu J *et al*. Covalent Modification of a Glassy Carbon Surface by 4-Aminobenzoic Acid and Its Application in Fabrication of a Polyoxometalates-Consisting Monolayer and Multilayer Langmuir. 2000, 16, 7471-7476.
(9) Arnold F. Metal-Affinity separations: a new dimension in protein processing. Nature Biotechnology. 1991, 9, 151-156.

## Acknowledgements

The authors would like to thank Jonathon Wagner and Dr. Ji Wu for helpful discussions. The authors would like to thank funding source of NIH, NSF and the department of CME and CeNSE at Univ. of KY.

**Bruce J. Hinds***

**bjhinds@uw.edu**

**Zhiqiang Chen (Phd 2014, Bristol-Myers Squibb)**